Electrochemical Properties of Hydrogen Absorbing Zintl Phases

Undergraduate Research Thesis

Presented in Partial Fulfillment of the Requirements for graduation "with Honors Research Distinction in Chemistry" in the undergraduate colleges of The Ohio State University

by

R. Dominic Ross

The Ohio State University

April 2018

Project Advisor: Professor Joshua Goldberger, Department of Chemistry and Biochemistry

Table of Contents

Acknowledgements

I would like to express my greatest appreciation to all the members of the Goldberger Group that have served as teachers and mentors to me over my several years of undergraduate research. In particular, to Dr. Maxx Arguilla and Dr. Nicholas Cultrara for their contributions to my project, as well as their teaching, help, and guidance in my undergraduate research. Furthermore, I would also like to thank Mr. Michael Scudder, Dr. Daniel Weber, and Mr. Zachary Baum for their various insights and assistance throughout the course of my time in the Goldberger Group. Most of all, I would like to thank Dr. Josh Goldberger for giving me the opportunity to do incredible research, and for his many hours advising my research and my career.

Vita

Education

Dublin Jerome High School……..2014

The Ohio State University, B.S. Chemistry……..2018

Honors and Awards

- Honors Arts & Sciences Undergraduate Research Scholarship (2017-2018)
- Booth Scholarship (2017-2018)
- Chellis Family Scholarship (2016-2017)
- Summer Undergraduate Research Fellowship (Summer 2016)
- MacNevin Memorial Scholarship (2015-2016)

Publications

4. Cultrara, N.D.; Arguilla, M.Q.; Jiang, S.; Sun, C.; Scudder, M.R.; Ross, R.D.; Goldberger, J.E. Group-13 and Group-15 Doping of Germanane. *Beilstein J. Nanotechnol* **2017,** 8, 1642-1648.

3. Aguilla, M.Q.; Cultrara, Scudder, M.R.; Jiang, S.; Ross, R.D.; Goldberger, J.E. Optical Properties and Raman-Active Phonon Modes in Two-Dimensional Honeycomb Zintl Phases. *Journal of Materials C* **2017**.

2. Arguilla, M.Q.; Cultrara, N.D.; Baum, Z.J.; Jiang, S.; Ross, R.D.; Goldberger, J.E. $EuSn_2As_2$: An Exfoliatable Layered Zintl-Klemm Phase. *Inorganic Chemistry Frontiers* **2017,** 4, 378-386.

1. Arguilla, M.Q.; Katoch, J.; Krymowski K.; Cultrara, N.; Xu, J.; Xi, X.; Hanks, A.; Jiang, S.; Ross, R.D.; Koch, R.J.; Ulstrup, S.; Bostwick, A.; Jozwiak, C.; Rotenberg, E.; McComb, D.; Shan, J.; Windl, W.; Kawakami, R.K.; Goldberger, J.E. $NaSn_2As_2$: An Exfoliatable Layered van der Waals Zintl Phase. *ACS Nano* **2016,** 10, 9500-9508.

List of Figures

Abstract

Novel, low-cost catalysts are needed for electrocatalysis for a wide variety of applications in order to move towards a renewable energy economy based on clean production and conversion of hydrogen. To date, most common catalysts have depended on pure precious metals or alloying some amount of a precious metals, restricting the commercialization of hydrogen fuel cell technologies. Here, we propose and explore the possibility of using Zintl phase catalysts as potential low-cost electrocatalysts, and using these measurements to understand the electrochemical mechanisms of this family of materials. Known Zintl phases GdGa and $BaGa_2$, each of which are known to be capable of hydrogenation to hydride phases, were synthesized using traditional solid state methods for this study, and confirmed by X-Ray Diffraction. Electrochemical measurements were taken using cyclic voltammetry. Platinum was measured at several pHs as a standard for hydrogen evolution reaction (HER) catalysis. As expected, platinum catalysis revealed high activity and low overpotential, but these properties rapidly decrease as a function of proton concentration. GdGa was measured at pH = 3, and was found to have the same slope as $BaGa_2$ at both pH = 5 and pH = 7, although these trends were distinct from the electrochemistry in the same region of the carbon substrate they were measured on (at pH = 3). This led to an investigation of the interaction of $BaGa_2$ in organic solvent with trimethylamine (TEA), a sacrificial hydrogen donor for possible electrochemical hydrogenation routes. $BaGa_2$ was revealed to reduce the irreversible oxidation potential of TEA from ~0.6 V vs. $Ag/AgNO_3$ to ~0.1 V vs. $AgAgNO_3$. Our results suggest that while the Zintl phases studied thus far do not have HER or OER catalysis ability, they may be useful for the electrochemical catalysis of organic reactions and may be able to be manipulated electrochemically.

Chapter 1: Introduction

1.1: Background

In recent years, the need for affordable, energy efficient catalysis has risen to the forefront of science as demand for low-cost and more environmentally conscious alternatives to fossil fuels grows. Currently, devices such as proton exchange membrane fuel cells (PEMFCs) and solar photovoltaic fuel cells require loading of platinum catalysts on at least one of the cell's half reactions. For the viability of a renewable energy based hydrogen economy, making the generation and subsequent oxidation of hydrogen energetically viable is vital. The low abundance of platinum, coupled with increasing demand for renewable energy production, has led to a rapid increase in the cost of platinum. Furthermore, while platinum has high activity for the hydrogen evolution reaction (HER), high loading (roughly 0.4 mg/cm^2)[1] remains necessary for the oxygen reduction reaction (ORR), the cathodic reaction in PEMFCs. Platinum already sees widespread industrial use as a high surface area catalyst for catalytic converters, and the demand for high activity catalysts to catalyze both half reactions in solar fuel cells and PEMFCs. For the anode reaction of PEMFCs, the hydrogen oxidation reaction (HOR), another costly precious metal, palladium, is also common. In spite of these concerns, research into non-precious metal electrocatalysis has remained sparse, despite some efforts that have not matched precious metals.[2,3,4,5]

In order to develop an economy that depends completely on hydrogen fuel, non-precious metal catalysts are necessary to make solar fuel cells (Figure 1) viable for routine use. There are a

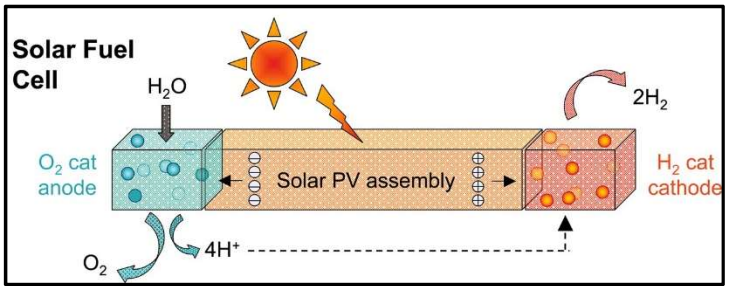

Figure 1 A schematic of a solar fuel cell. The cathode (left) is the oxygen evolution reaction (OER) and the cathode (right) is the hydrogen evolution reaction (HER).[6]

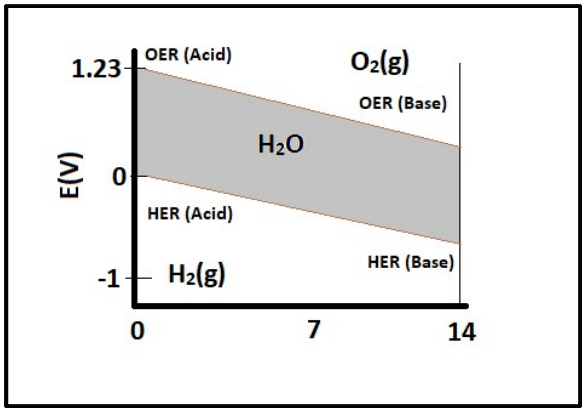

Figure 2 Pourbaix diagram of water stability (not to scale) where the slope of the borders of water stability are 59.2 mV/pH unit.

variety of potential device architectures, but most basically, HER provides a method to produce hydrogen without the production of greenhouse gases and using solar energy in a photoelectrochemical cell with OER at the anode and HER at the cathode.[7] By lowering the necessary overpotential of the anode half reaction (OER) and the cathode half reaction (HER), hydrogen could pose a solution to the difficulty of storing renewable energy sources that are only intermittently available, such as wind and solar energy. Ultimately, hydrogen energy provides a clear pathway to a worldwide economy based entirely on clean energy, but the ability to efficiently generate it for storage from renewable energy and subsequently transform the energy stored in hydrogen bonds back into usable energy.[8,9]

Catalysts are vital to making both production of hydrogen for storage and conversion of stored hydrogen into electricity both economically, environmentally, and energetically viable. By finding efficient non-precious catalysts for both oxygen and hydrogen catalysis, each of these goals is possible.

HER in Acidic Media:
$H^+ + e^- \rightarrow H_{ads}$
$H_{ads} + H_{ads} \rightarrow H_2$ (Tafel)
$H_{ads} + H^+ + e^- \rightarrow H_2$ (Heyrovsky)

HER in Basic Media:
$H_2O + e^- \rightarrow H_{ads} + OH^-$
$H_{ads} + H_{ads} \rightarrow H_2$ (Tafel)
$H_{ads} + H_2O + e^- \rightarrow H_2 + OH^-$ (Heyrovsky)

ORR in Acidic Media:
$O_2 + 4H^+ + 4e^- \rightarrow H_2O$
$O_2 + 2H^+ + 2e^- \rightarrow H_2O_2$
$H_2O_2 + 2H^+ + 2e^- \rightarrow 2H_2O$

ORR in Basic Media:
$O_2 + H_2O + 4e^- \rightarrow 4OH^-$
$O_2 + H_2O + 2e^- \rightarrow HO_2^- + OH^-$
$HO_2^- + H_2O + 2e^- \rightarrow 3OH^-$

Figure 3 Mechanistic steps of common reactions of interest for electrochemical catalysis.

HER is expected at potentials of 0 V vs. the reversible hydrogen electrode (RHE) given that the definition of the reference electrode is defined for this potential. OER is expected at a theoretical potential of 1.23 V, and will

thus be expected to occur at this potential or greater. However, some amount of overpotential, or the amount of energy above the thermodynamic theoretical potential required to drive the reaction, is always required. Platinum catalysts generally have near zero overpotential for HER/HOR, but ORR/OER remains a challenge, and cost remains an issue.

1.2: Zintl Phases and Zintl Phase Hydrogenation

Zintl phases are a family of materials consisting of at least one element from Group 1 or Group 2 (or from the lanthanides), and at least one element from Group 13, 14 or 15. These materials exhibit complete electron donation from electropositive atoms to covalently bonded networks of more electronegative atoms. These materials have been demonstrated to have a wide number of applications and interesting properties, including use as thermoelectrics[10], superconductors[11], and 2D devices[12]. To date, few Zintl phase catalayst have been studied, and no Zintl phase electrocatalysts have been studied.

Many Zintl phases exhibit the ability to absorb hydrogen into their crystal structures to form hydride phases. For example, GdGa can be hydrogenated at high pressure to form a mixture of polyanionic hydrides $GdGaH_{1.66}$.[13] $BaGa_2$ forms the polyanionic hydride $BaGa_2H_2$.[14] In polyanionic hydrides, the hydrogens act as covalently bonded terminal ligands to the

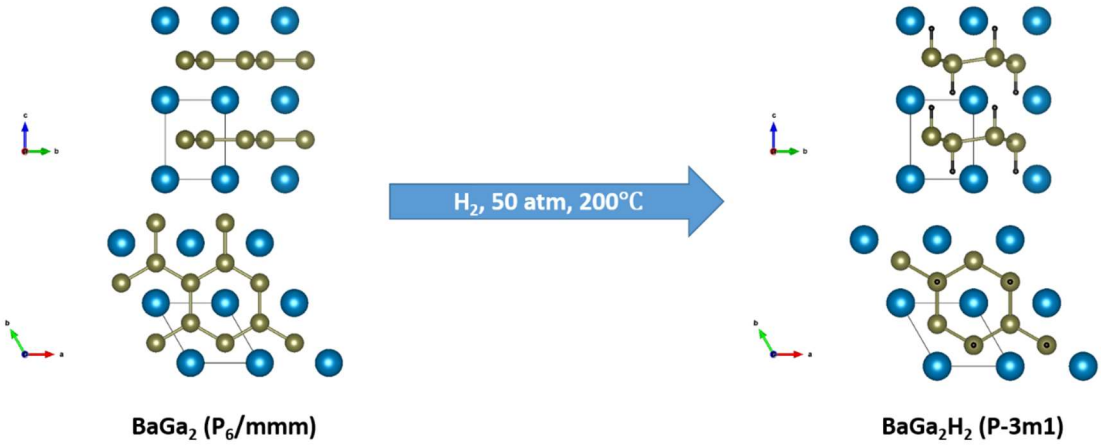

Figure 4 High presssure hydrogenation scheme of $BaGa_2$ from Hausserman. Blue = barium, green = gallium, black = hydrogen.

electronegative elements (in the case of $GdGaH_{1.66}$ and $BaGa_2$, the gallium). However, Zintl phases may also form interstitial hydrides, where hydrogens are formally negative and coordinated by the less electronegative alkali, alkaline earth, or rare earth element.[15] These different bonding schemes occurring in these materials gives materials even with seemingly similar characteristics a vast array of electronic and structural properties. Many different Zintl phases with and without hydrides are already known in the literature: a small catalogue of some Zintl phases of interest are shown in Table 1.[16]

Table 1 Some selected Zintl phases of interest for eventual study, exemplifying the different amounts of hydrogen uptake for different phases.

Phase	Hydrogenation
GdGa (Cmcm)	GdGaH and $GdGaH_{1.66}$
$GdGa_2$ (P6/mmm)	Does not hydrogenate
$SrAl_2$ (Fd-3m O1)	$SrAl_2H_2$ (air sensitive)
$BaGa_2$ (P6/mmm)	$BaGa_2H_2$
$SrGa_2$ (P6/mmm)	$SrGa_2H_2$
BaGaGe (P6/mmm)	BaGaGeH
BaInGe (P-3m1)	BaInGeH
$BaIn_2$ (Imma)	Does not hydrogenate
$BaSn_2$ (P-3m1)	Does not hydrogenate
EuSi (Cmcm)	$EuSiH_{1.8}$
BaGaSn	BaGaSnH

1.3: Zintl Phase Electrochemistry

Zintl phases are of interest for studying hydrogen catalysis due to the large catalogue of related phases with different affinities for uptake of hydrogen into their crystal lattices, and the wide variation of different properties, including their ability, or lack thereof, to uptake hydrogen amongst them. As shown in Figure 5, transition metal catalysts have wildly varying hydrogen catalysis activity. This comes from their ability to bind hydrogen to their surface, expressed in terms of $\Delta G_{H^\bullet}$, or the theoretical adsorption free energy of a hydrogen onto the material surface. Materials with a high adsorption energy necessary to bind to the surface, such as silver, will not energetically favor the process, and there's never the chance for HER catalysis to proceed. However, when this free energy is too greatly negative, hydrogens essentially become trapped on the surface of the material, and either lead to sluggish kinetics or the halt the process entirely. The breadth of the larger family of Zintl phases, as well as the potential to form various hydrides from these phases, make the hydrogenatable Zintl phases and their analogues a promising class of materials for finding a non-precious material with this "ideal" hydrogen adsorption energy. Still, to date, the Zintl phases' electrochemical properties and electrocatalysis remains largely unexplored, and no Zintl phase electrocatalysts have been previously demonstrated.

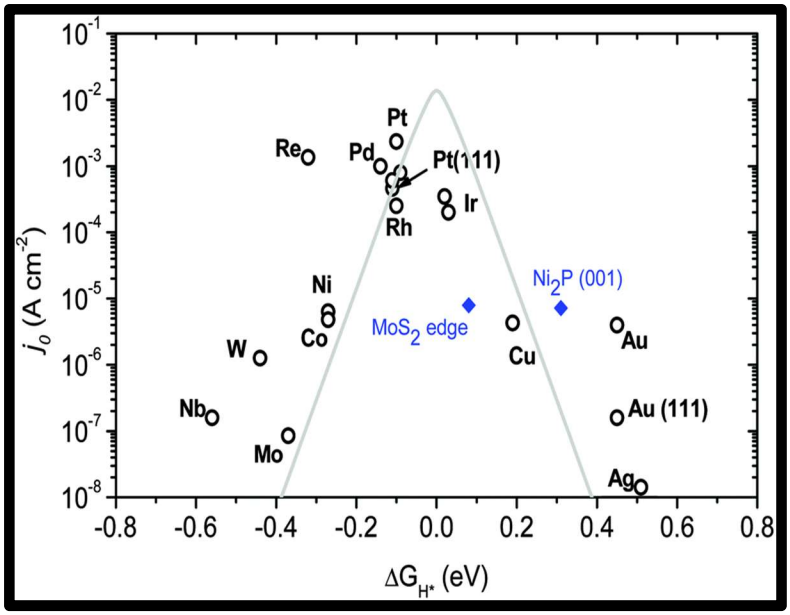

Figure 5 The so-called "volcano plot" of various transition metal catalysts plotted with their exchange current current density as a function of free energy of hydrogen absorption.[17]

Building up a "library" of the catalytic interactions of many Zintl phases will also allow for building up a "volcano plot" for Zintl phases and Zintl phase hydrides. This would allow for comparison of the trends in these materials to known transition metal catalysts as well as well characterized non-precious metal catalysts, such as MoS_2. Understanding the varying catalytic activity of Zintl phases versus their hydride phases could also elucidate if and how catalysis proceeds in these materials.

To further explore the possible electrochemical transformations of Zintl phases and investigate new alternatives to traditional solid state routes to obtaining Zintl phase hydrides, the possibility of reducing protons electrochemically to diffuse into the Zintl phase precursor crystal structure is being investigated.

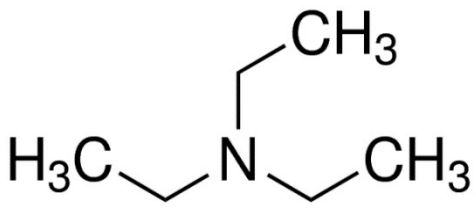

Figure 6 Triethylamine structure.

Triethylamine (TEA) is a known "sacrificial-hydrogen" donor, meaning that is able to donate hydrogens at the cost of undergoing an irreversible oxidation. Sacrificial donors are attractive for their ability to release protons in non-aqueous media under more mild conditions where Zintl phases are stable. The oxidative process is also irreversible, making it an ideal material to electrochemically react without the possibility of kinetics pushing the reaction backwards. These organic molecules have been suggested as potential candidates for methods to induce solar energy harvesting in certain types of solar cells.[18] Here, we hope to demonstrate that electrochemically induced irreversible oxidation of the TEA sacrificial donor can selectively induce the reaction of $BaGa_2$ with protons and electrons to form $BaGa_2H_2$, as envisioned in the scheme below.

$$BaGa_2 + 2e^- + 2H^+ \rightarrow BaGa_2H_2$$

$$TEA \rightarrow H^+ + TEA^- + 2e^-$$

Ultimately, we hope to apply fixed potentials to $BaGa_2$ bulk electrodes on extended timescales in order to demonstrate by XRD, Raman, and FTIR/DRIFTS measurements that structural changes from the change in crystal structure due to the addition of hydrogen in the lattice, and the presence of Ga-H bonding.

Chapter 2: Materials Synthesis and Characterization

2.1: Synthesis of Zintl Phase Precursor Materials

Initial synthetic efforts attempted the synthesis of Zintl phase precursors from loading stoichiometric amounts of the pure elements in evacuated quartz ampoules. Use of stoichiometric loading of gadolinium and gallium in ampoules with furnace heating and slow cooling lead to products highly impure with the eutectic $GdGa_2$ phase.

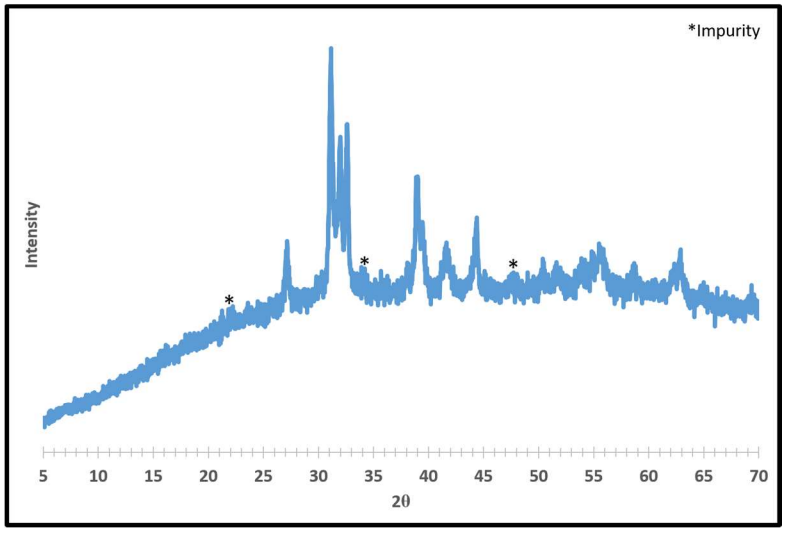

Figure 7 Powder X-Ray Diffraction pattern of GdGa labeled with synthetic conditions.

GdGa was synthesized by arc melting gallium droplets and a 2% excess of pressed pellets of gadolinium powder in a copper hearth. After the initial melt, the product was flipped over, returned to the arc melter, and re-melted. This process was repeated to result in five total flips of the material. The synthesis was completed at the scale to obtain approximately a gram of final product.

$BaGa_2$ was synthesized by loading stoichiometric amounts of barium pieces and gallium droplets in an alumina crucible inside an evacuated quartz ampoule, then heating for 12 hours at 900°C. The synthesis was completed at the scale to obtain approximately a gram of final product.

2.2: Solid Characterization of Zintl Phase Precursors

X-Ray Diffraction characterization was used to confirm phase purity of each of the Zintl phase samples. Confirmation scans, shown in Figures 6 and 7, were performed on a Rigaku Miniflex II spectrometer. While they are mostly pure, achieving complete phase purity is

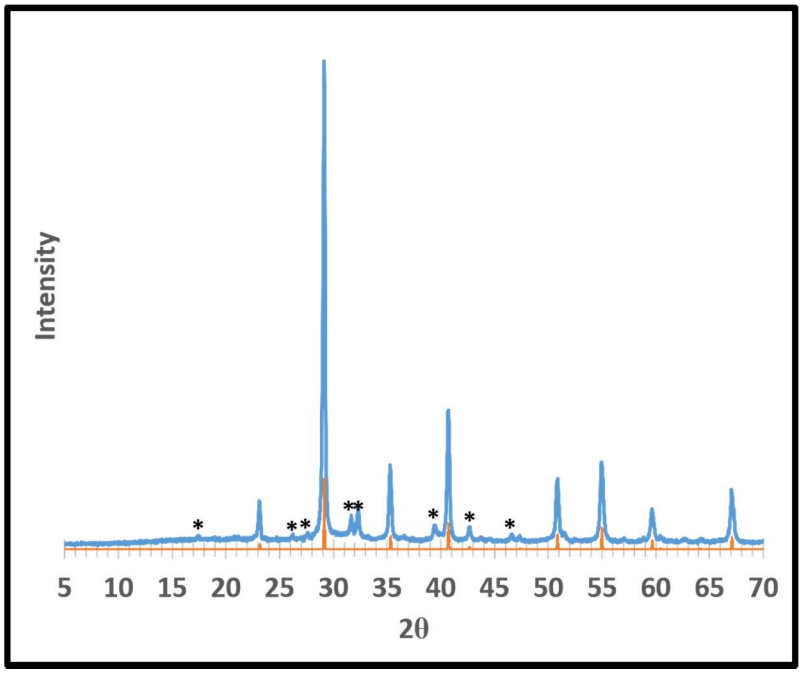

Figure 8 Powder X-Ray Diffraction pattern of $BaGa_2$. Impurity ($BaGa_4$) peaks are labeled with asterisks.

difficult due to the presence of eutectic phases of $GdGa_2$ and $BaGa_4$, readily forming in favor of GdGa and $BaGa_2$, respectively.

Chapter 3: Electrocatalysis

3.1: Platinum Catalysis Setup and ECSA Analysis

In order to benchmark the performance of Zintl phase catalysts at different potentials and at various pH. Standards were collected at pH = 1, pH = 3, pH = 5, and pH = 7. Due to extremely low signal in dilute concentrations of protons, the standards of pH = 5 and pH = 7 are not shown or analyzed here. These measurements were all taken on a CHI760D or a CHI604D potentiostat, using cyclic voltammetry (CV) techniques.

Platinum electrodes were prepared by preparing dispersions of carbon black and platinum black in solvent, and then drop-casting baking them onto glassy carbon electrodes. The dispersions were prepared by sonication of approximately 1:2 by mass platinum black:carbon black in approximately 10 mL of distilled water. These suspensions were then ultrasonicated for 15 minutes before addition of a dilute solution of Nafion to bind the carbon to the platinum, then ultrasonicated further. Immediately after removal from sonication, the solution is dropcast onto glassy carbon rotating disk electrodes, then left to bake on in an oven for 1.5 hours.

Platinum catalysts were measured in solutions of $HClO_4$ electrolyte. The working electrode was a glassy carbon electrode with the deposition of Pt/C, the counter electrode was a platinum wire, and the reference electrode was a reversible hydrogen electrode using a platinum wire. The electrolyte solution was bubbled with N_2 for 20 minutes prior to, and during, measurements. All electrolyte solutions used were set at an ionic strength of $\mu = 0.1$ M by the addition of $NaClO_4$, if necessary. These measurements were all taken on a CHI760D or a CHI604D potentiostat. Cyclic voltammetry experiments for HER were taken at a scan rate of 100 mV/s, and data shown represents the final cycle measured unless otherwise noted.

For calculation of the electrochemically active surface area (ECSA), the charge in the capacitive double layer region of the cyclic voltammetry plot was used to manually integrate total charge of the double layer, which was converted to the ECSA of platinum. The double layer region was taken to be 0.4 V – 0.5 V for pH = 1, and 0.4 V – 0.482 V for pH = 3. Capacitive currents were found by taking the average of negative currents (the bottom current points of the CV) and the average of the positive currents (the top current points of the CV) for a steady state cycle. Then, the magnitude of the difference between the capacitive current and each current point is calculated – this value is then averaged for each two adjacent points, and divided by the scan rate (step size) to give the current generated between the two points.

$$Q_2 = \frac{|I_c - I_1| + |I_c - I_2|}{2v}$$

Equation 1. v is scan rate of a cyclic voltammetry measurement (V), I_c is the average capacitive current from either the positive or negative region of the scan (A), and I_1 and I_2 are two arbitrary current points (A). Q_2 is the charge calculated from two given current points (C).

The literature value of the electrochemically active surface area of platinum has been found to be 210 μC/cm^2.[19] This value is used to convert the integrated charge from a cyclic voltammetry plot into an amount of surface area. Calculating the ECSA allows for normalization of CV plots to current density (mA/cm^2) as opposed to just current, and allows for establishing consistency between different electrodes of the same material.

3.2: Zintl Phase Electrocatalysis Setup

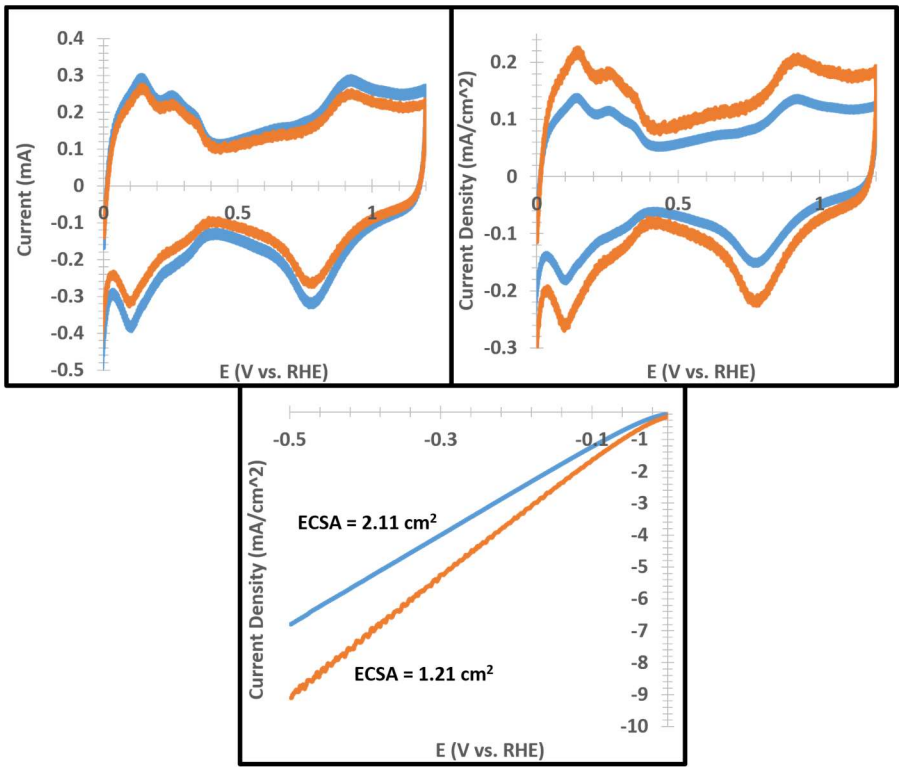

Figure 9. Experimentally collected platinum black CV data before (top left) and after (top right) normalization, and the normalized HER region data shown on the bottom.

To begin measuring the electrocatalytic activity of Zintl phases, the process of baking platinum electrodes was replicated as closely as possible. Zintl phase catalysts were measured in solutions of $HClO_4$ electrolyte. The working electrode was a glassy carbon electrode with the deposition of Zintl phase/C, the counter electrode was a platinum wire, and the reference electrode was a reversible hydrogen electrode using a platinum wire. The electrolyte solution was bubbled with N_2 for 20 minutes prior to, and during, measurements. All electrolyte solutions used were set at an ionic strength of $\mu = 0.1$ M by the addition of $NaClO_4$. These measurements were all taken on a CHI760D or a CHI604D potentiostat. Cyclic voltammetry experiments for HER were taken at a scan rate of 100 mV/s, and data shown represents the final cycle measured unless otherwise noted.

GdGa was found to visibly dissolve in solutions of acid at pH values below pH = 3. Thus, electrolyte solutions for GdGa were first prepared at pH = 3. GdGa was observed to not suspend well in pure water, instead aggregating at the bottom of the solvent container. To remedy this,

GdGa and carbon black were dispersed in solutions of 20% water by mass in methanol. Approximately a 1:1 mass ratio of GdGa:carbon black was used due to the high molecular weight of GdGa. These were each added to the water/methanol mixture, then ultrasonicated for 15 minutes, followed by the addition of 40 μL Nafion binder solution, and then further sonication. These dispersions were also dropcast onto RDEs and left to bake for 1.5 hours.

$BaGa_2$ was observed to bubble in acidic solutions below pH = 5. Thus, electrolyte solutions for $BaGa_2$ catalysis measurements were prepared at pH = 5 and pH = 7 to study HER. $BaGa_2$ electrodes were made on glassy carbon using the same procedure as described for GdGa, and with the same measurement conditions.

3.3: pH = 3 (GdGa and Platinum on Carbon)

Compared to the pH = 1 data, platinum had significant lower activity (nearly an order of magnitude lower current density) at the same overpotential values. GdGa does show a similar curve shape to this platinum trend, albeit as much higher onset overpotentials, and with a smaller apparent Tafel slope. Similar to platinum, there does appear to be two distinct regions of electrochemistry, suggesting two different active surface facets of GdGa, or the consequence of diffusion limitation at pHs above 1. In GdGa, the first is a mild onset near -0.75 V, and the second is a much sharper onset just below -1.5 V.

GdGa has an observed cycle dependence, i.e. more current is observed at a given overpotential after more CV cycles. The change in activity suggests some electrochemical change in the GdGa material. Either there is a degradation or transformation to another material (such as a more active hydride phase), or there is another material taking up surface sites on the

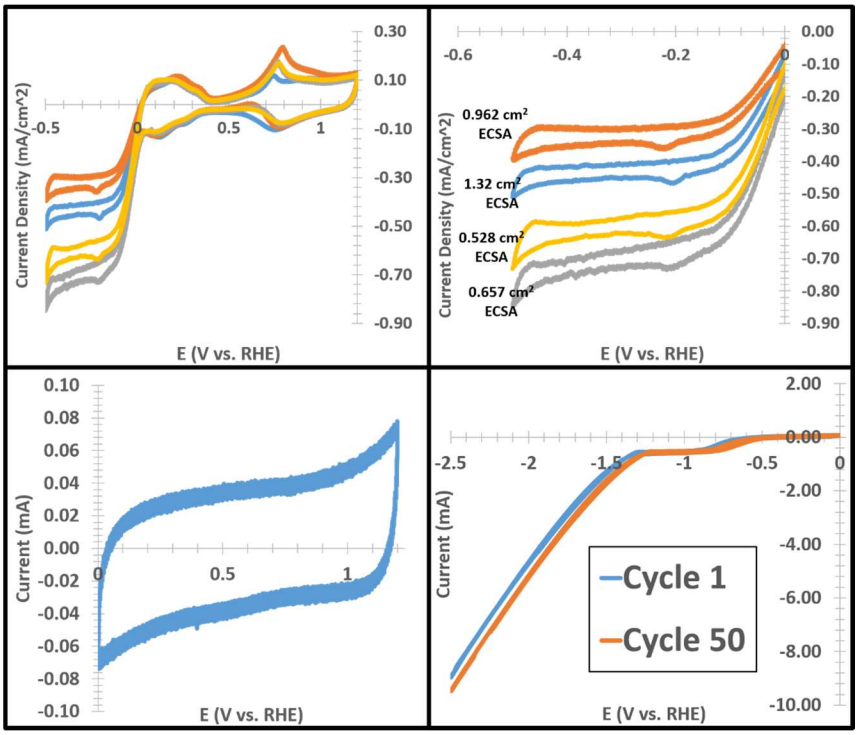

Figure 10 Top left: Normalized CV plot of platinum on carbon in pH = 3 $HClO_4$ electrolye solution. Top right: Inset of platinum CV at pH = 3 highlighting the HER region. Bottom left: Capacitance region of GdGa CV at pH = 3. Bottom right: GdGa CV in HER region.

GdGa. Literature suggests the latter is the case.[20] Recent work has suggested that use of a platinum counter electrode for HER measurements can lead to the formation of platinum nanodots on the surface of the working electrode material. Thus, this cycle dependence likely arises from the formation of the platinum nanodots taking up GdGa active sites and leading to greater electrochemical activity at these sites.

3.4: pH = 5 ($BaGa_2$ and Platinum on Carbon)

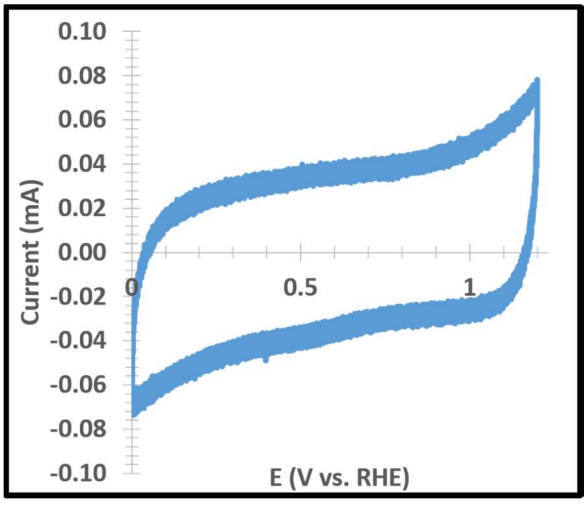

Figure 11 Capacitance region of $BaGa_2$ measured at pH = 5.

Platinum standards were measured for pH = 5. However, appreciable current was not able to be observed using the same setup as the other HER measurements. pH = 5 results for platinum are thus not displayed. $BaGa_2$ measurements were replicated as described above at the new pH, and the results are further discussed below.

3.5: pH Dependence of Zintl Phase Electrochemistry and pH = 7 ($BaGa_2$ and Platinum) and pH = 12 ($BaGa_2$ and Gold)

Platinum standards were measured for pH = 7. However, appreciable current was not able to be observed using the same setup as the other HER measurements. pH = 7 results for platinum are thus not displayed. The pH = 7 results of $BaGa_2$ are instead shown in comparison to the previously displayed pH = 5 $BaGa_2$ results. Given that the shape of the curve in the HER region and the absolute current is nearly identical for both $BaGa_2$ at pH = 5 and pH = 7, this suggests a lack of dependence on the concentration of protons in solution. If HER was occurring in this potential range, then current would be proportional to the decrease in pH, as it is with platinum. Since the HER mechanisms described earlier depend on protons, current should increase, as

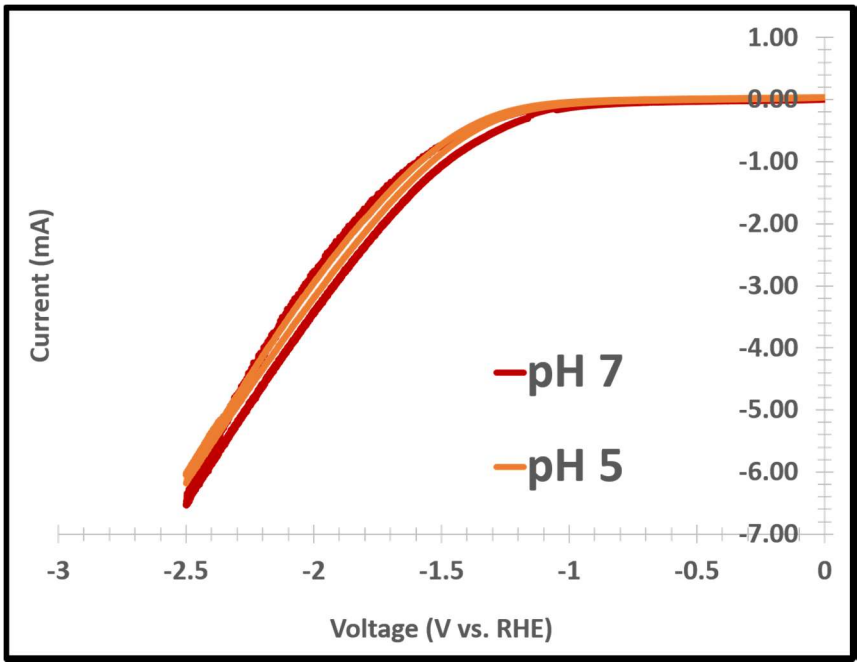

Figure 12 $BaGa_2$ CV plot in the HER region at pH = 5 and pH = 7.

there are more of the species available to be reduced. However, this isn't the case, which means the electrochemistry occurring with $BaGa_2$ on carbon does not depend on protons and therefore is not HER.

As seen in Figure 13, GdGa displays the same trend as $BaGa_2$ at pH = 5. These are each also compared against a carbon black deposition that was prepared with the same electrode dropcast preparation method described earlier, but no platinum or Zintl phase material was added. The carbon black on glassy carbon electrode was then by CV measured at pH = 3. While current in the HER region does occur, it clearly follows a different trend than $BaGa_2$ (pH = 5) and GdGa (pH = 3).

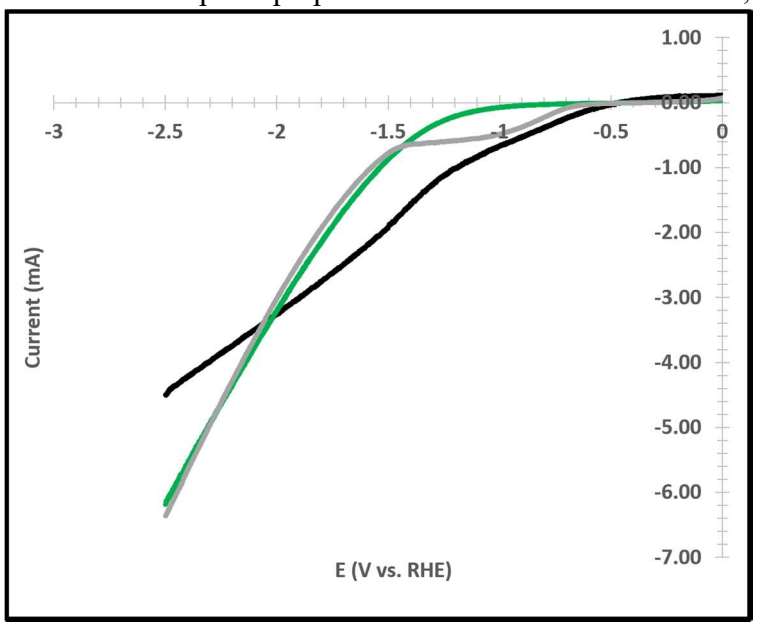

Figure 13 CV plot displaying $BaGa_2$ in (pH = 5) in green, GdGa (pH = 3) in gray, and carbon black (pH = 3) in black, revealing the presence of non-pH dependent electrochemistry that is common to these two Zintl phase, and distinct from the substrate.

$BaGa_2$ was also measured in a solution of pH = 12 KOH with an ionic strength of $\mu = 0.1$ M. However, across four measurements of $BaGa_2$ electrodes, $BaGa_2$ had no appreciable signal when compared to a gold standard. It appears although it doesn't immediately dissolve or bubble in base, the basic solution strips away the surface of the $BaGa_2$ electrode over time, particularly when a potential is cycled.

GdGa and $BaGa_2$ each follow an extremely similar trend in the HER region, however, even at different pH values. This suggests that a non-HER, non-hydrogen dependent process is occurring that is not caused by the substrate. The only major difference observed between GdGa and $BaGa_2$ occurs near -0.75 V, where GdGa has a current peak before the major onset of the current slope. This could indicate the presence of minor catalytic activity in GdGa, or may simply indicate an additional electrochemically active surface facet that isn't present in $BaGa_2$. However, this may also be a consequence of a diffusion limitation at higher pHs with more dilute concentrations of protons. Regardless, their onset of a major slope downward in current just

before -1.5 V suggest that the non-pH dependent feature in $BaGa_2$ is also present in GdGa, likely indicating an electrochemical reduction unique to these Zintl phases. Further study would be needed to reveal whether this generalizes to other similar Zintl phases. Given that they are non-catalytic in nature, some reduction of the Zintl phase materials must be occurring. The use of XPS or bulk electrochemical transformations of Zintl phase electrodes could also allow for tracking any structural changes occurring within the Zintl phase electrodes during this reduction.

Chapter 4: Electrochemical Hydrogenation

Electrochemical hydrogenation experiments were performed using a Gamry Reference 600 Potentiostat/Galvanostat instrument. The working electrode was a glassy carbon disk electrode, the counter electrode was a platinum disk electrode, and the reference electrode was a $Ag/AgNO_3$ non-aqueous reference electrode in acetonitrile. All measurements used 0.1 M $LiClO_4$ as a supporting electrolyte in acetonitrile. Before measurement, solutions were bubbled through with nitrogen. All scan ranges for this experiment were set to -3 V to 3 V, but are cut off at the points where the current begins spiking.

The presence of a cyclic voltammetry peak near 0.63 V in the the CV plot of TEA in acetonitrile suggests that this oxidative potential of TEA in acetonitrile, given that no other major events appear in the CV plots of TEA in acetonitrile, and the oxidation peak of TEA is expected to be irreversible. TEA in acetonitrile clearly displays a difference in potential between the major positive potential event that occurs in the CV of acetonitrile before the addition of TEA, suggesting that the observed spike in current must be due to electrochemistry involving the TEA, and not the solvent.

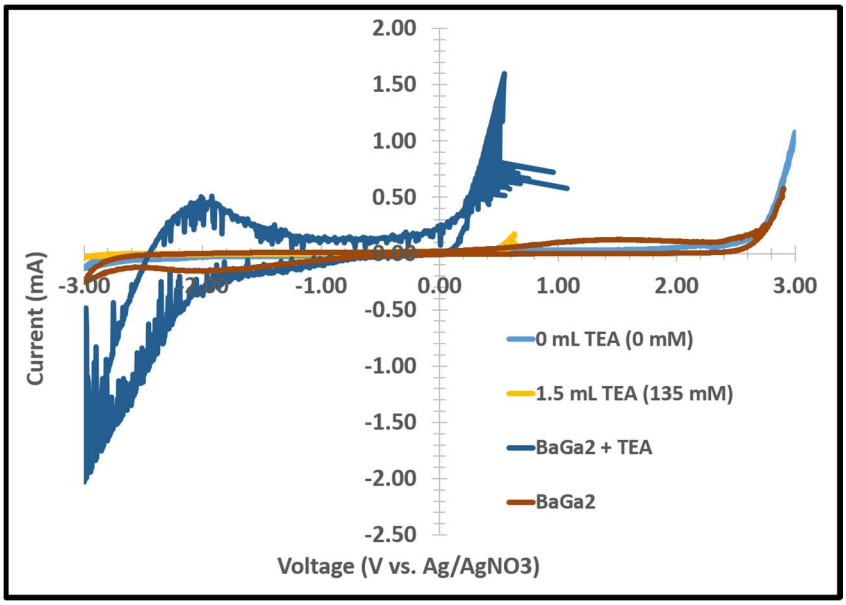

Figure 14 Cyclic voltammetry plots of acetonitrile with a glassy carbon electrode with varied TEA concentration, with and without $BaGa_2$ deposition on the glassy carbon surface.

When the glassy carbon electrode was switched out for the $BaGa_2$ on carbon electrode, there are notable electrochemical feature changes. Perhaps most notably, the observed CV peak at 0.63 V with the TEA in acetonitrile solution has shifted to an onset at nearly 0.1 V.

This peak appears unique to the interaction of $BaGa_2$ with TEA, since it does not appear in the TEA or $BaGa_2$ CV. This suggests that either electrochemistry unique to the combination of the two phases is occurring. There also doesn't appear to be a symmetric peak in the CV for this event, suggesting that this is likely still the TEA oxidation occurring at a lower potential, and $BaGa_2$ could be a catalyst for the electrochemical oxidation of TEA in acetonitrile. This would entail TEA is losing protons and electrons to the environment – further measurement would be needed to see if any stoichiometric transformation of the $BaGa_2$ has also occurred, or if the $BaGa_2$ acts catalytically. The other possibility would be that acetonitrile is being reduced, while the $BaGa_2$ is preserved as a catalyst. The appearance of a pair of reduction and oxidation events in the negative region that were not present in the other CVs suggests that new molecules may be formed in this process.

Chapter 5: Conclusions

Despite the lack of promise for electrochemical hydrogen evolution catalysis based on the two phases studied thus far, there is a great deal of work to be done in the electrochemical characterization of Zintl phases. The work done so far suggests that GdGa and $BaGa_2$ share non-hydrogen dependent common electrochemical reductions. Other Zintl phases may also exhibit different catalytic behavior that is still important to elucidate the mechanism of catalysis in non-precious metal catalysts. Measuring $GdGa_2$ and $BaGa_4$ could elucidate the reasons for the lacking electrocatalytic performance of $BaGa_2$ and GdGa should these more thermodynamically stable phases prove more electrocatalytically active. Synthesizing Zintl phase hydrides and studying how the electronic and structural changes due to hydrogen uptake affect electrochemistry will also allow for larger generalizations of how Zintl phases interact with hydrogen, and point towards future non-precious material candidates for hydrogen and oxygen catalysis. Understanding the electrochemical pathways common to Zintl phases could lead to a high throughput, scalable route to Zintl phase hydrides.

Preliminary work in the electrochemical hydrogenation of $BaGa_2$ also suggests that $BaGa_2$ could be a catalyst for the oxidation of TEA. If this is the case, $BaGa_2$ could a be a useful catalyst for light-harvesting in three-component artificial photosynthesis systems.

Further work will continue to benchmark various Zintl phase catalysts and their Zintl phase hydrides, as well as exploring the mechanisms of catalysis by active sites by Brunauer-Emmett-Teller (BET) gas adsorption measurements, bulk electrochemical transformations of $BaGa_2$ (and other Zintl phase) electrodes, and surface characterization (XPS, SEM).

References

1. Shao, M.; Chang, Q.; Dodelet, J.P.; Chenitz, R. Recent Advances in Catalysts for the Oxygen Reduction Reaction. *J. Chem. Rev.* **2016**, 116, 3594-3657.

2. Benck, J.; Hellstern, T.R.; Kibsgaard, J.; Chakthranont, P.; Jaramillo, T.F. Catalyzing the Hydrogen Evolution Reaction (HER) with Molybdenum Sulfide Nanomaterials. *ACS Catalysis.* **2014,** 4, 3957-3971.

3. Lee, J.G.; Hwang, J.; Hwang, H.J.; Jeon, O.S.; Jang, J.; Kwon, O.; Lee, Y.; Han, B.; Shul, Y.G. A New Family of Perovskite Catalysts for Oxygen-Evolution Reaction in Alkaline Media: $BaNiO_3$ and $BaNi_{0.83}O_{2.5}$. *J. Am. Chem. Soc.* **2016,** 138 (10), 3541-3547.

4. Tan, S. M.; Chua, C.K.; Sedmidubsky, D.; Sofer, Z.; Pumera, M. Electrochemistry of layered GaSe and GeS: applications to ORR, OER, and HER. *Phys. Chem. Chem. Phys.* **2015,** 18, 1699-1711.

5. Li, Y.; Wang, H.; Xie, L.; Liang, Y.; Hong, G.; Dai, H. MoS_2 Nanoparticles Grown on Graphene: An Advanced Catalyst for the Hydrogen Evolution Reaction. *J. Am. Soc.* **2011,** 133, 7296-7299.

6. N.S. Lewis, D.G. Nocera. Powering the planet: Chemical Challenges in solar energy utilization. *PNAS*. **2006**, 103, 15729-15735.

7. Walter, M.; Warren, E.; McKone, J.R.; Boettcher, S.W.; Mi, Q.; Santori, E.A.; Lewis, N.S. Solar Water Splitting Cells. *Chem. Rev.* **2010,** 110, 6446-6473.

8. Maeda, K.; Domen, K. Photocatalytic Water Splitting: Recent Progress and Future Challenges. *J. Phys. Chem. Lett.* **2010**, 1, 2655-2661.

9. Yilanci, A.; Dincer, I.; Ozturk, H.K. A review on solar-hydrogen/fuel cell hybrid energy systems for stationary applications. *Progress in Energy and Combustion Science***. 2009**, 35, 231-244.

10. Kauzlarich, S.M.; Brown, S.R.; Snyder, G.J. Zintl phases for thermoelectric devices. *Dalton Transactions.* **2007**, 2099-2107.

11. Goto, Y.; Yamada, A.; Matsuda, T.D.; Mizuguchi, Y. SnAs-Based Layered Superconductor $NaSn_2As_2$. *J. Phys. Soc. Jpn.* **2017**, 86, 123701.

12. Arguilla, M.Q.; Katoch, J.; Krymowski K.; Cultrara, N.; Xu, J.; Xi, X.; Hanks, A.; Jiang, S.; Ross, R.D.; Koch, R.J.; Ulstrup, S.; Bostwick, A.; Jozwiak, C.; Rotenberg, E.; McComb, D.; Shan, J.; Windl, W.; Kawakami, R.K.; Goldberger, J.E. $NaSn_2As_2$: An Exfoliatable Layered van der Waals Zintl Phase. *ACS Nano* **2016,** 10, 9500-9508.

13. Nedumkandathil, R.; Kranak, V.F.; Johansson, R.; Angstrom, J.; Balmes, O.; Andersson, M.S.; Nordblad, P.; Scheicher, R.H.; Sahlberg, M.; Häussermann, U. Hydrogenation induced structure and property changes in GdGa. *J. Solid State Chem.* **2016,** 239, 184-191.

14. Lee, M.H.; Evans, M.J.; Daemen, L.L.; Sankey, O.F.; Häussermann, U. Vibrational Property Study of $SrGa_2H_2$ and $BaGa_2H_2$ by Inelastic Neutron Scattering and First Principles Calculations. **2008,** 47, 1496-1501.

15. Häussermann, U.; Kranak, V.F.; Puhakainen, K. Hydrogenous Zintl Phases: Interstitial Versus Polyanionic Hydrides. *Struct Bond*. **2011**, 139, 143-162.

16. Bjorling, T. Synthesis and characterization of Zintl hydrides. Doctoral Thesis, Stockholm University, 2008.

17. Guio-Morales, C.G.; Stern, L.A.; Hu, X. Nanostructured hydrotreating catalysts for electrochemical hydrogen evolution. *Chem. Soc. Rev.* **2014**, 43, 6555-6569.

18. Pellegrin, Y.; Odobel, F. Sacrificial electron donor reagents for solar fuel production. *Comptes Rendus Chimie.* **2017**, 20, 283-295.

19. Sheppard, S.A.; Campbell, S.A.; Smith, J.R.; Lloyd, G.W.; Ralph, T.R.; Walsh, F.C. Electrochemical and microscopic characterisation of platinum-coated perfluorosulfonic acid (Nafion 117) materials. *Analyst.* **1998**, 123, 1923-1929.

20. Chen, R.; Yang, C.; Cai, W.; Wang, H.Y.; Miao, J.; Zhang, L.; Chen, S.; Liu, B. Use of Platinum as the Counter Electrode to Study the Activity of Nonprecious Metal Catalysts for the Hydrogen Evolution Reaction. *ACS Energy Letters*. **2017**, 2, 1070-1075.